International Journal for Housing Science and Its Applications
Publish August 3, 2025. Volume 46, Issue 3 Pages 558-573

https://doi.org/10.70517/ijhsa46340

Research on structural design and stability improvement of new power system energy storage network based on optimization algorithm

Wenbin Cai[1,*], Ye Li[1], Kaiyang Song[1], Wei Bai[1] and Yating Chen[1]
[1] Inner Mongolia Electric Power Economic and Technical Research Institute Branch, Inner Mongolia Electric Power (Group) Co., Ltd., Hohhot, Inner Mongolia, 010000, China
Corresponding authors: (e-mail: 18686016708@163.com).

Abstract In the process of constructing a new type of power system, energy storage configuration plays an important role in supporting the stable operation of a new type of power system mainly based on new energy. This paper constructs an optimization model with the constraints and optimization objectives of the optimal configuration of the new power system. The improved MOPSO algorithm is proposed to be written in Matlab language for model solving. The standard test functions ZDT1-ZDT4 are selected as test examples to verify the effectiveness and performance advantages of the proposed algorithm. The improved MOPSO algorithm and the typical multi-objective algorithms NSGA-II and MOSPO are evaluated by the multi-objective algorithm evaluation index. The test results show that the improved MOPSO algorithm has the best overall performance, and the Pareto front solution is more uniformly distributed and more diversified. Taking the IEEE-34 node system with wind/light/diesel/storage islanded grid topology selected as an example, the improved MOPSO algorithm is used to design the energy storage network structure and improve the system stability. The optimal access locations of energy storage are found to be nodes 834, 860, and 836, and the multi-storage configuration scheme designed in this paper improves the voltage stability by 77.96%. The research results have important theoretical and engineering value for exploring the optimal configuration scheme of energy storage in distribution networks.

Index Terms energy storage configuration, optimization model, MOPSO algorithm, new power system

I. Introduction

With the accelerated industrialization of human society and rapid economic development, the use of fossil energy is increasing, and the problems of environmental pollution and energy depletion have become difficult problems that need to be solved by various countries [1], [2]. Therefore, the development of renewable energy to replace fossil energy has become a major strategic policy in China. Although clean renewable energy sources such as solar and wind energy have been widely emphasized and have broad market potential, the problems of unstable supply and poor continuity during the use of such energy sources limit their further application and have certain limitations [3]-[5].

The power system, as a generation, distribution and transmission system, traditionally requires instantaneous generation and instantaneous power collection [6]. The current power energy storage technology is mainly combined by energy storage devices and power electronic components combined with energy conversion devices, which effectively improves the regional differences in power supply, peak and valley differences, seasonal differences, etc., and solves many national problems, which is particularly critical [7]-[9]. On the one hand, the establishment of large-capacity energy storage devices can be utilized for the effect of “peak and valley adjustment” in the power grid [10]. That is, by storing enough idle power during the low-power period at night, and then feeding back the stable output during the peak power period in the daytime, the utilization rate of power generation facilities can be greatly improved, and the country can save a huge amount of investment [11]-[13]. On the other hand, it plays an important role in improving power supply reliability and power quality [14]. In recent years, the development of clean energy such as wind and solar energy has been very rapid, but affected by seasonal, weather and regional conditions, it has obvious discontinuity and instability, with large fluctuations in power generation and poor adaptability [15], [16]. Energy storage technology can substantially solve the gap and volatility of wind and solar power generation, which can accomplish the stable transmission of power generation and scientifically adjust the fluctuation of the corresponding data of the power grid caused by power generation [17], [18]. Therefore, the design of high specific capacity power system energy storage network structure with high active material loading and stable mechanical properties has become an important direction of research [19], [20].

In this paper, the constraints of the energy storage system in terms of rated power, rated capacity, charging and discharging power, and charging state are sorted out, and the objectives of economy, reliability, and stability of the optimized energy storage configuration are studied in detail. Aiming at the multi-objective optimization problem of energy storage configuration in new power system, a method of optimizing energy storage configuration in distribution network based on multi-objective particle swarm optimization (MOPSO) algorithm is proposed. The MOPSO algorithm is used to solve the multi-objective energy storage configuration model, and an adaptive mutation strategy is introduced during the population update process to expand the particle's ability to explore the space, which effectively improves the diversity of the population while ensures late convergence, and obtains the globally optimal solution in the energy storage configuration problem. According to the analysis results, the energy storage network structure is redesigned to achieve the best optimal energy storage configuration.

II. Optimized design of new power system energy storage configuration

New energy can be recycled and regenerated, is environmentally friendly and non-polluting, has low operating costs and a wide geographical distribution. At the same time, new energy has uncertain volatility, unstable power generation, easy to cause power fluctuations and stability of the power system. In order to ensure the stable operation of the power system containing new energy, the power station must be equipped with energy storage equipment to smooth out the uncertain fluctuation of power generation [21]. How to configure energy storage equipment with the best economic and environmental benefits to ensure the stability and reliability of the new power system is of great significance to the development of new energy power industry.

This paper describes the constraints and optimization objectives of the optimal configuration of the new power energy storage system. For the multi-objective nonlinear planning problem of optimizing the energy storage configuration of the distribution network system, the model is solved using the improved MOPSO optimization algorithm. The installation nodes of energy storage are optimally configured to achieve the best optimal energy storage configuration scheme.

II. A.Mathematical model for optimal allocation of energy storage system

The clear constraints and optimization objectives are the basis for realizing efficient energy storage configuration, which can lay a theoretical foundation for the selection and application of subsequent solution algorithms.

II. A. 1) Constraints

(1) Rated power constraint

The energy storage power rating is the maximum power that an energy storage system can release or absorb per unit of time, which is a key indicator for evaluating its charging and discharging capability. This constraint is directly related to the charging and discharging capacity of the energy storage device, which is crucial for scenarios such as emergency response, load balancing, and renewable energy grid integration [22].

Let the time period of action be T, and the configured P_{rated} is related to the magnitude of energy storage output within T. Therefore, the P_{rated} constraint can be expressed as:

$$P_{rated} \geq \max\left\{\left|\max_{t\in(0,T)}\left[\Delta P_E(t)\right]\right|\eta_{ch}, \frac{\left|\min_{t\in(0,T)}\left[\Delta P_E(t)\right]\right|}{\eta_{dis}}\right\} \tag{1}$$

where: η_{ch}, η_{dis} are the charging and discharging efficiencies of the energy storage device, respectively. The $\Delta P_{\mathrm{E}}(t)$ is the output power of the energy storage at the moment of Y.

(2) Rated capacity constraint

The rated capacity of the energy storage, on the other hand, is the maximum amount of electricity that can be stored by the energy storage system, usually expressed in kWh. This constraint is very critical for the continuous power supply capability of the system and affects the effective use of the energy storage device during peak load.

Let Q_{SOC} denote the energy storage charge state, the rated capacity constraint of energy storage can be expressed as:

$$E_{rated} \geq \max\left\{\frac{\max\left(\int_0^{k\Delta T} P_E(t)dt\right)}{Q_{\max}-Q_0}, \frac{-\min\left(\int_0^{k\Delta T} P_E(t)dt\right)}{Q_0-Q_{\min}}\right\} \tag{2}$$

where: E_{rated} is the rated capacity of the energy storage. Q_0 is the charge state of the energy storage at the initial moment. $Q_{\min}$, $Q_{\max}$ are the minimum and maximum charging state of the energy storage, respectively.

(3) Charge/discharge power constraint

During the operation of the energy storage system, the charging and discharging power constraints are the key factors affecting its performance and stability. Charging and discharging power constraints mainly refer to the maximum and minimum power limits that can be achieved by the energy storage device during charging and discharging.

The charging power constraint indicates the maximum energy that the energy storage can absorb in a specific time, while the discharging power constraint indicates the maximum energy that the energy storage can release in a specific time [23], expressed as:

$$\begin{cases} P_{ch,t,\max} = \min\left[P_{rated}, \dfrac{(Q_{\max}-Q_{SOC,t})E_{rated}}{\eta_{ch}\Delta t}\right] \\ 0 \leq P_{ch,t} \leq P_{ch,t,\max} \end{cases} \tag{3}$$

$$\begin{cases} P_{dis,t,\max} = \max\left[-P_{rated}, \dfrac{(Q_{\min}-Q_{SOC,t})E_{rated}\eta_{dis}}{\Delta t}\right] \\ P_{dis,t,\max} \leq P_{dis,t} \leq 0 \end{cases} \tag{4}$$

where: Δt is the charge/discharge time of the stored energy. $Q_{\mathrm{SOC},t}$ is the charge state of the energy storage at t. $P_{\mathrm{ch,t}}$, $P_{\mathrm{dis,t}}$ are the charging power and discharging power at t moment, respectively. $P_{ch,t,\max}$, $P_{dis,t,\max}$ are the maximum charging power and discharging power at t moment, respectively.

(4) Charge state constraints

In the optimal allocation scheme of energy storage capacity, a reasonable range of charging state needs to be set.

The expression of the energy storage charging state constraint is:

$$Q_{\min} \leq Q_{soc.t} \leq Q_{\max} \tag{5}$$

$$Q_{high} - Q_{low} \geq 0 \tag{6}$$

$$Q_{SOC.t} = Q_{SOC.t-1} + \frac{1}{E_{rated}}\left(\eta_{ch}P_{cht} - \frac{P_{dis.t}}{\eta_{dis}}\right)\Delta t \tag{7}$$

where: Q_{high}, Q_{low} are the larger and smaller values of the energy storage charge state, respectively.

II. A. 2) Optimization objectives

Since the positive role of energy storage in power system operation mainly involves economy, stability and reliability, the optimization objectives of energy storage configuration are divided into economy, stability and reliability objectives.

(1) Economic objectives

The economic objective is the key index of the optimized configuration of energy storage. By constructing the mathematical model of investment cost and operation cost of energy storage, minimizing the investment and operation cost and maximizing the operation benefit can be taken as the optimization goal, and through scientific calculation and analysis, the reasonable configuration of energy storage system can be realized.

1) Investment cost

The investment cost of energy storage is mainly composed of initial investment cost and replacement investment cost. The initial investment cost usually involves the cost of equipment procurement, installation and system integration, while the replacement investment cost includes the cost of equipment renewal and maintenance. Since the rated power and rated capacity of an energy storage system determine the size and performance of the energy storage system, the rated power and rated capacity become important factors affecting the initial investment cost.

The initial investment cost of energy storage over the whole life cycle is:

$$C_c = C_{PCS} P_{rated} \tag{8}$$

where: C_{PCS} is the unit power cost of the power conversion system. P_{rated} is the rated power of the energy storage.

The replacement investment cost expression is:

$$C_z = \sum_{i=0}^{n} C_{bat} E_{rated} (1+r)^{-[iT_{LCC}/(n+1)]} \tag{9}$$

where: C_{bat} is the unit capacity cost. r is the discount rate. T_{LCC} is the energy storage life cycle. n is the number of replacement times (total input energy storage $(n+1)$ times), $n = T_{LCC} / T_{Life}$, and T_{Life} is the equivalent cyclic life of energy storage.

Therefore, the expression for the total cost of energy storage full life cycle investment is:

$$C_{inv} = C_c + C_{z'} \tag{10}$$

2) Operating costs

The operation cost of energy storage mainly includes operation and maintenance cost and end-of-life treatment cost. The energy storage operation and maintenance cost expression is:

$$\begin{aligned} C_{OM} &= C_{POM} P_{rated} \left\{ \left[(1+r)^{T_{LCC}} - 1 \right] \Big/ \left[r(1+r)^{T_{LCC}} \right] \right\} \\ &+ \sum_{t=1}^{T_{LCC}} C_{EOM} W(t) (1+r)^{-t} \end{aligned} \tag{11}$$

where: C_{POM} is the operation and maintenance cost per unit of power. P_{rated} is the rated power of energy storage. C_{EOM} is the operation and maintenance cost per unit capacity. $W(t)$ is the annual charge/discharge amount of energy storage (1 year charge/discharge time is calculated according to 300d).

The energy storage end-of-life treatment cost expression is:

$$C_{sd} = C_{Psd} P_{rated} (1+r)^{T_{LCC}} + \sum_{j=1}^{n+1} C_{Esd} E_{rated} (1+r)^{-jT_{LCC}/(n+1)} \tag{12}$$

where: C_{Psd} is the end-of-life treatment cost per unit of power. C_{Esd} is the end-of-life treatment cost per unit capacity.

In summary, the cost of energy storage based on the whole life cycle cost is:

$$C_{LCC} = C_{inv} + C_{OM} + C_{sd} \tag{13}$$

(2) Stability objectives

New energy power generation has uncertainty, in the event of power generation system failure or power shortage, it is necessary to equip a reasonable capacity of energy storage system to continue to provide users with electricity to meet the load demand for a certain period of time, and power fluctuations to meet the limit requirements to ensure the stability of the operation of the power grid system. Through energy storage devices, power can be stored during low demand periods and released during peak hours, ensuring that users have access to a stable power supply at all times.

This process can be affected by two key metrics: outage time and outage frequency. Outage time refers to the total length of power interruption experienced by customers, while outage frequency indicates the number of outage events that occur. An efficient energy storage system not only significantly reduces the duration and frequency of outages, but also improves the overall resilience and stability of the grid, providing users with a more stable power experience.

The average frequency of outages occurring:

$$E_a = \frac{\sum_{y=1}^{Y}\sum_{i=1}^{N_d} N_i b_{i,y}}{Y\sum_{i=1}^{N_d} N_i} \tag{14}$$

where: y is the current year. N_d is the number of nodes in the power system. N_i is the number of users at node i. $b_{i,y}$ is the number of outages that occurred on node i in year y. Y is the total number of years for which the statistics are computed.

The average duration of outages occurred:

$$E_b = \frac{\sum_{y=1}^{Y}\sum_{i=1}^{N_d} N_i U_{i,y}}{Y\sum_{i=1}^{N_d} N_i} \tag{15}$$

where: $U_{i,y}$ is the time of occurrence of blackout at node i in year y.

Average stable continuous power supply rate:

$$E_c = 1 - \frac{\sum_{y=1}^{Y}\sum_{i=1}^{N_d} N_i U_{i,y}}{8760Y\sum_{i=1}^{N_d} N_i} \tag{16}$$

(3) Reliability objective

The reliability objective of energy storage configuration optimization aims to ensure that under any operating scenario, the power system is able to stably and continuously provide sufficient and reliable power to fully satisfy the electricity demand of users, and effectively avoid the risk of insufficient or interrupted power supply.

Power shortage is also a key indicator of concern, which refers to the failure of the energy storage system to meet the load demand, and its corresponding time probability of power shortage and time expectation of power shortage help to assess the performance of the system and its ability to cope with sudden load growth. The adequacy of power security can effectively reduce the risk of power supply, improve the resilience of the overall power system, and provide users with a reliable power supply environment.

Power supply shortage expectation number:

$$E_d = \frac{\sum_{y=1}^{Y}\sum_{i=1}^{N_d} L_{i,y}}{Y} \tag{17}$$

where: $L_{i,y}$ is the amount of outage load at node i in year y.

The time probability of power supply shortage is as follows:

$$L = \sum_{k} p_k t_k \tag{18}$$

where: p_k is the probability when the out-of-service load quantity occurs. t_k is the duration of time when the out-of-service load quantity occurs.

Electricity supply shortage time expectation:

$$E_f = \sum_{i=1}^{m}\sum_{j=1}^{n_i} p\left(X \geq (C_i - L_{ij})\right) \tag{19}$$

where: m is the number of time periods in the year. n_i is the number of days in the i th time period. L_{ij} is the peak load on the j th day in the i th time period. C_i is the installed capacity of the system in the i th time period.

Electricity supply shortage time expectation:

$$E_p = \sum_{i=1}^{m}\sum_{j=1}^{n_i}\sum_{k=1}^{24}\sum_{X=C_i-L_{ijk}}^{C_i}\left(X-(C_i-L_{ijk})\right)P_{ijk}\left(X\right) \tag{20}$$

where: P_{ijk} is the outage load greater than X probability at the K hour of the j th day in the i th time period. L_{ijk} is the load at the K th hour of the j th day in the i th time period.

II. B.Solution algorithm for optimal allocation of energy storage system

For the multi-objective nonlinear planning problem of energy storage allocation optimization in distribution network system, this paper uses MOPSO algorithm to solve the model. The standard MOPSO algorithm has the advantages of simple parameters and fast convergence speed, but there are the following problems when solving the multi-objective energy storage allocation optimization problem.

(1) In the face of multi-dimensional problems, its Pareto optimal solution is not well distributed.

(2) The social cognition of particles tends to make the particles gather too quickly, so that they lose the diversity of the population and fall into local optimality.

(3) The position of initialized particles has a greater impact on the convergence speed and accuracy of the algorithm and the presentation of the final results. The root of the problem is that the particles do not explore the solution space comprehensively enough. Therefore, this paper introduces an adaptive mutation strategy into the population updating process of the standard MOPSO to expand the exploration ability of the particles on the space, which improves the diversity of the population and ensures the late convergence at the same time.

II. B. 1) Standard MOPSO algorithm

Compared with the global optimal solution searched by traditional particle swarm algorithms, MOPSO pursues non-inferior solutions and seeks the Pareto-optimal solution set by analyzing its dominance relationship. According to the inertia, individual cognition and social cognition of the particles [24], the updating formulas of their velocity and position are as follows:

$$v_i(t+1) = wv_i(t) + c_1r_1(x_{pbest,i}(t) - x_i(t)) + c_2r_2(x_{gbest}(t) - x_i(t)) \tag{21}$$

$$x_i(t+1) = x_i(t) + v_i(t+1) \tag{22}$$

$$w(t) = w_{\max} - \frac{w_{\max} - w_{\min}}{t_{\max}} \times t \tag{23}$$

where: i is the particle number. t is the current iteration number. $x_{\text{pbest},i}(t)$ is the individual best position of particle i iterated to the t th generation. $x_{\text{gbest}}(t)$ is the global best position of the population particle iteration to the t th generation. c_1, c_2 are the individual and global learning factors, which are generally between 0 and 2. r_1, r_2 are random constants from 0-1. w is the inertia weight, which usually decreases with the number of iterations to enhance convergence. $w_{\max}$, $w_{\min}$ are upper and lower bounds on the inertia weights, respectively. The $t_{\max}$ is the maximum number of iterations.

II. B. 2) Adaptive mutation strategies

In order to improve the ability of the particle population to globally explore the solution space and overcome the problem that traditional particle swarm algorithms are prone to fall into the local optimum, a stochastic variation operator is added to the basic framework of the algorithm, which improves the ability of the particle swarm algorithm to jump out of the local optimum solution by randomly varying the intergenerational global optimum position x_{gbest}, so that the algorithm is able to enter the solution space when precocious convergence happens to continue searching in other regions of the solution space until a globally optimal solution is finally found.

As a result, let f_i be the fitness (objective function value) of the i th particle, then the average fitness f_{avg} of the entire population of n particles can be found according to equation (24). Then, the particle swarm normalization calibration factor f is determined according to Eq. (25), then the population adaptation variance σ^2 of the whole population can be obtained according to Eq. (26).

$$f_{avg} = \frac{1}{n}\sum_{i=1}^{n} f_i \tag{24}$$

$$f = \begin{cases} \max\left\{\left|f_i - f_{avg}\right|\right\} & \max\left\{\left|f_i - f_{avg}\right|\right\} > 1 \\ 1 & Other \end{cases} \tag{25}$$

$$\sigma^2 = \sum_{i=1}^{n}\left(\frac{f_i - f_{avg}}{f}\right)^2 \tag{26}$$

For x_{gbest} that satisfy the mutation condition to mutate with a certain probability p_{m}, p_{m} is calculated as follows:

$$p_m = \begin{cases} u & \sigma^2 < \sigma_d^2 \ And \ f\left(x_{gbest}\right) > f_d \\ 0 & Other \end{cases} \tag{27}$$

where: u is a random number between 0.1 and 0.3. The value of σ_{d}^2 is generally much smaller than the maximum value of σ^2. The f_{d} can be set to the theoretical optimum. For the variational operation of x_{gbest}, the method of adding random perturbations is used, and $x_{\mathrm{gbest},i}$ is set to be the i th $dimensional fetch of x_{gbest}, and η is the random variable obeying the distribution of $Gauss\left(0,1\right)$, which is:

$$x_{gbest,i} = x_{gbest,i}\left(1 + 0.5\eta\right) \tag{28}$$

II. C.Model solving process

In this paper, the improved MOPSO algorithm is written in Matlab language for simulation based on the optimization model constructed in Eq. (1) to Eq. (28). The decision variable consists of the location of the two energy storage, the capacity size and its charging and discharging power at each moment in a day, with a total of 52 dimensions. Firstly, the charging and discharging power and its location information within a day are randomly generated according to the constraints of the storage charging and discharging power and its position constraints in the network in Eqs. (3) and (4), and then the rated capacity of the energy storage is obtained by using the maximum interval method of Eq. (1) and the SOC curves are obtained by obtaining the capacity and the SOC curves for each moment of the energy storage system according to Eq. According to Eq. (2), the capacity of each moment of the energy storage system is obtained to obtain the SOC curve and determine whether it satisfies the constraints. Taking the IEEE-34 node system selected by wind/light/diesel/storage islanded grid topology as an example, the network topology of IEEE-34 nodes is modified in real time accordingly and Matpower is called to carry out the trend calculation, and the three objective function values are minimized as the quantitative assessment indexes to judge whether the current scheme is good or bad, and the improved MOPSO algorithm iterates repeatedly on the control variables to ultimately obtain the optimal access location of the energy storage. Optimal access location. The node topology of wind/light/diesel/storage islanded grid is shown in Fig. 1.

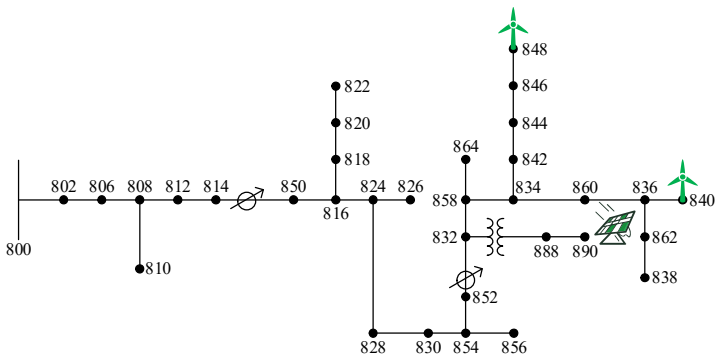

Figure 1: Topography of wind/solar/diesel/ESS isolated microgrid

III. Empirical analysis

The study takes the optimal allocation of energy storage in wind/light/diesel/storage islanded grid as an example, solves the mathematical model of optimal allocation of energy storage system based on the improved MOPSO algorithm, and adjusts the structure of energy storage network according to the results of energy storage allocation.

III. A. Algorithm performance testing and evaluation analysis

III. A. 1) Multi-objective test functions

In order to test the effectiveness of the proposed improved MOPSO algorithm and its performance advantages and disadvantages, this paper selects the most representative international typical test functions ZDT1-ZDT4 as the test instances for validation and evaluation. The expressions and properties of the adopted dual-objective test functions ZDT1-ZDT4 are shown below:

$$ZDT1:\begin{cases}\min f_1(x)=x_1\\ \min f_2(x)=g\left(1-\sqrt{x_1/g}\right)\\ g(x)=1+9\left(\sum_{i=2}^{m}x_i/(n-1)\right)\\ s.t.0\le x_i\le 1,i=1,2,\cdots,30\end{cases} \tag{29}$$

$$ZDT2:\begin{cases}\min f_1(x)=x_1\\ \min f_2(x)=g\left[1-\left(\sqrt{x_1/g}\right)^2\right]\\ g(x)=1+9\left(\sum_{i=2}^{m}x_i/(n-1)\right)\\ s.t.0\le x_i\le 1,i=1,2,\cdots,30\end{cases} \tag{30}$$

$$ZDT3:\begin{cases}\min f_1(x)=x_1\\ \min f_2(x)=g\left(1-\sqrt{x_1/g}\right)-x_1\sin\left(10\pi x_1\right)/g\\ g(x)=1+9\left(\sum_{i=2}^{m}x_i/(n-1)\right)\\ s.t.0\le x_i\le 1,i=1,2,\cdots,30\end{cases} \tag{31}$$

$$ZDT4:\begin{cases}\min f_1(x)=x_1\\ \min f_2(x)=g\left(1-\sqrt{x_1/g}\right)\\ g(x)=1+10(n-1)+\sum_{i=2}^{m}\left(x_i^2-10\cos(4\pi x_i)\right)\\ s.t.0\le x_1\le 1,-5\le x_i\le 5,i=2,\cdots,30\end{cases} \tag{32}$$

III. A. 2) Optimization algorithm evaluation metrics

The evaluation metrics for the performance of multi-objective algorithms are divided into three main categories: metrics for assessing the approximation of the approximate Pareto front obtained by the algorithm to the real Pareto front (convergence metric generation distance GD), metrics for assessing the diversity and homogeneity of the set of approximate solutions (diversity metrics, spatial measure metrics SP), and metrics for combining the convergence and diversity of the set of approximate solutions (inverse generation distance IGD, hypervolume indicator HV) [25]. The following three metrics were selected for evaluation.

(1) GD

Generation distance (GD), as one of the convergence metrics, is usually used to measure the degree of approximation between the approximate solution set generated by the algorithm solution and the real Pareto front. Where the smaller GD value indicates that the approximate solution set is closer to the true Pareto frontier, and the better the performance of the algorithm. When GD is 0 it means that the generated solution set is completely coincident with the real Pareto front, i.e., the generated solution is the optimal solution. Its calculation formula is as follows:

$$GD = \frac{\sqrt{\sum_{i=1}^{N} d_i^2}}{N} \tag{33}$$

where: N denotes the number of non-dominated solutions in the true Pareto front. d_i denotes the Euclidean distance from the i th approximate solution to the reference point in the real Pareto front.

(2) SP

The spacing metric (SP), as one of the common metrics for evaluating the diversity and uniformity of the distribution of nondominated solutions in the Pareto front, is usually used to measure the average distance between neighboring solutions in the Pareto front, which is computed by the following formula:

$$SP = \sqrt{\frac{1}{N-1}\sum_{i=1}^{N}\left(\bar{d} - d_i\right)^2} \tag{34}$$

where: $d_i = \min\left(\sum_{m=1}^{M}\left|f_m(x_i) - f_m(x_j)\right| i, j = 1,2,\cdots,N, i \neq j\right)$. N denotes the number of non-inferior solutions obtained by the algorithm. d_i denotes the minimum distance between the objective value of the i th non-inferior solution and the objective values of all other non-inferior solutions. $\bar{d}$ denotes the average of the minimum distances obtained. M denotes the number of objective functions. Where, the smaller the value of SP, the more uniformly the solution set on the Pareto front is distributed and the better the diversity is.

(3) IGD

Inverse Generation Distance (IGD) is a comprehensive index to evaluate the convergence and diversity of the multi-objective algorithm, which represents the average value of the Euclidean distance from the reference point x to the approximate solution y on the real Pareto front, and its calculation formula is as follows:

$$IGD = \frac{\sum_{y \in P^*} \min_{x \in P} d(x,y)}{\left|P^*\right|} \tag{35}$$

$$d(x,y) = \min_{j=1}^{|P^*|} \sqrt{\sum_{m=1}^{M} \frac{f_m(p_i) - f_m\left(p_j^*\right)^2}{f_m^{\max} - f_m^{\min}}} \tag{36}$$

where $P = \left\{p_1, p_2, \cdots, p_{|P|}\right\}$ denotes the set of approximate solutions solved by the algorithm, and $P^* = \left\{p_1^*, p_2^*, \cdots, p_{|P^*|}^*\right\}$ denotes a set of reference points uniformly adopted on the real Pareto front. $d(x,y)$ is the Euclidean distance between the reference point x on P^* and the point y on P . $f_m^{\max}$ and $f_m^{\min}$ denote the maximum and minimum values of the m th objective in the real Pareto solution set, respectively. Smaller IGD values indicate that the generated approximate solution set is closer to the real Pareto front, and the algorithm has better convergence and non-inferior solution diversity.

III. A. 3) Analysis of test results

In order to verify the performance of the proposed improved MOPSO algorithm, the distribution of the optimal solution sets obtained by different algorithms on the optimal frontier is compared and analyzed, and the comparison algorithms are the proposed improved MOPSO and the typical multi-objective algorithms NSGA-II and MOSPO, respectively, and the population size of the three algorithms is set to 200, and the size of the external document is

100, and the three algorithms are based on the same test function. ZDT1-ZDT4 were run separately for 30 times to find out the mean (MEA) and standard deviation (STD) of different evaluation indexes mentioned above.

The convergence metrics GD value, SP value and IGD value of different algorithms on the test functions ZDT1-ZDT4 are shown in Tables 1 to 3, respectively. Where bolding indicates the minimum value of different multi-objective algorithms on the test function. The mean and standard deviation values of convergence metrics GD, SP and IGD of the proposed improved MOPSO algorithm on test functions ZDT1-ZDT4 are significantly better than the other algorithms.

Table 1: Algorithms are the GD of the convergence of the test function ZDT1-ZDT4

Test function		Improved-MOPSO	MOPSO	NSGA-II
ZDT1	MEA	4.54E-04	4.38E-03	3.93E-02
	STD	4.79E-05	4.72E-03	3.53E-02
ZDT2	MEA	1.17E-05	2.48E-03	3.16E-03
	STD	1.73E-04	1.73E-03	4.99E-03
ZDT3	MEA	1.34E-04	1.61E-02	3.08E-02
	STD	1.88E-04	2.83E-02	3.55E-02
ZDT4	MEA	3.73E-05	1.54E-02	3.04E-02
	STD	3.29E-04	1.15E+00	2.46E+00

Table 2: Algorithms are the SP of the convergence of the test function ZDT1-ZDT4

Test function		Improved-MOPSO	MOPSO	NSGA-II
ZDT1	MEA	1.31E-04	2.98E-01	1.11E-01
	STD	4.16E-04	1.11E-01	4.25E-01
ZDT2	MEA	3.22E-04	4.46E-02	2.65E-02
	STD	3.85E-05	2.7E-02	1.81E-02
ZDT3	MEA	2.82E-04	1.86E+00	3.54E+00
	STD	1.73E-05	3.58E+00	1.02E+00
ZDT4	MEA	1.03E-04	1.98E-02	1.72E-02
	STD	3.9E-05	3.7E-02	1.57E-02

Table 3: Algorithms are the IGD of the convergence of the test function ZDT1-ZDT4

Test function		Improved-MOPSO	MOPSO	NSGA-II
ZDT1	MEA	4.47E-05	3.12E-01	2.77E-01
	STD	4.85E-04	2.86E-01	1.67E-01
ZDT2	MEA	4.89E-04	2.66E-03	1.95E-03
	STD	3.16E-05	3.44E-03	2.84E-03
ZDT3	MEA	4.79E-04	3.53E-02	3.28E-02
	STD	3.42E-05	1.78E-01	4.7E-01
ZDT4	MEA	4.93E-04	2.41E-01	1.49E-01
	STD	4.22E-05	1.84E-01	3.76E-01

The Pareto approximation frontiers obtained by the three different algorithms on the test function ZDT1 are shown in Fig. 2. (a)~(c) denote the distribution of Pareto fronts for the MOPSO algorithm, the NSGA-II algorithm, and the improved MOPSO algorithm, respectively (same below). The experimental simulation results show that the Pareto front of the test function ZDT1 is concave and continuous, and the algorithm (c) proposed in this paper outperforms both the traditional MOPSO (a) and the classical NSGA-II algorithm (b) in terms of the effect of the test function of ZDT1, and the obtained set of approximate solutions very closely approximates the real Pareto optimal front, which has the best convergence performance and diversity, and the external file also has the best uniformity of the non-inferior solutions with good spatialization, in contrast to the NSGA-II algorithm which is the worst in convergence and the distribution of the non-inferior solutions in the solution space obtained by the classical MOSPO algorithm.

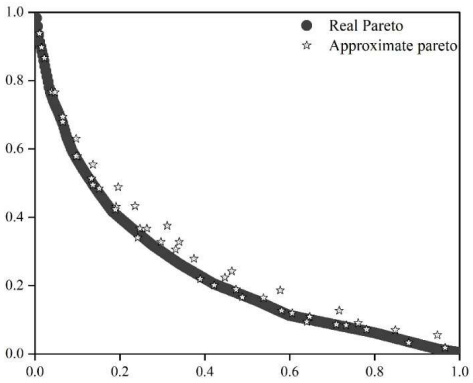

(a) MOPSO

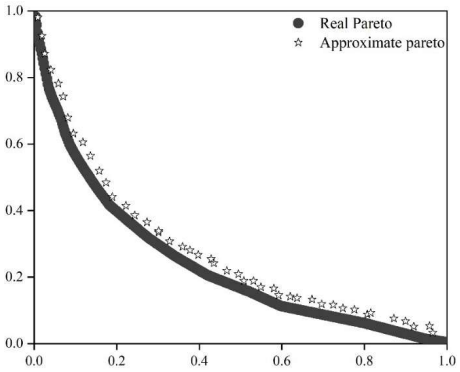

(b) NSGA-II

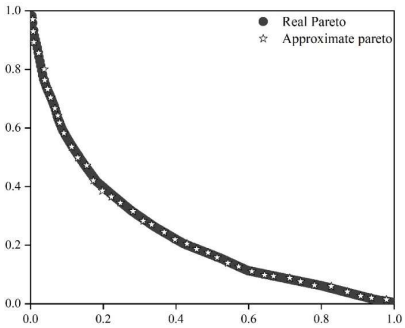

(c) Improved-MOPSO

Figure 2: The algorithm is near the edge of the pareto approximation on ZDT1

The Pareto approximation frontiers obtained by the three different algorithms on the test function ZDT2 are shown in Fig. 3. It can be seen that the Pareto front of the test function ZDT2 is convex and continuous, and the algorithm proposed in this paper (c) outperforms both the traditional MOPSO (a) and the classical NSGA-II algorithm (b) in terms of the effectiveness of the test function ZDT2, in contrast, the non-inferiority solution obtained by the traditional MOSPO algorithm has the worst uniformity in the spatial target distribution. The non-inferiority solution obtained by the NSGAII algorithm deviate the most from the true Pareto frontier reference, and the algorithm proposed in this paper has the best convergence and diversity performance, as well as the best uniformity of non-inferior solutions in the external archive.

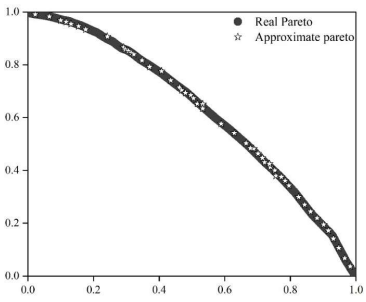

(a) MOPSO

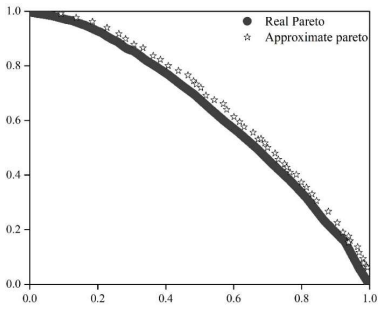

(b) NSGA-II

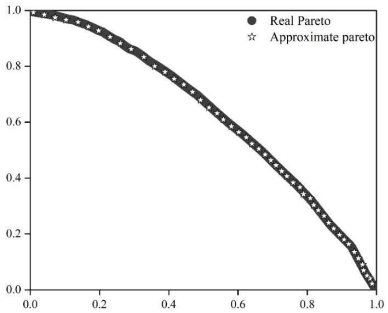

(c) Improved-MOPSO

Figure 3: The algorithm is near the edge of the pareto approximation on ZDT2

The Pareto approximation frontier obtained by three different algorithms on the test function ZDT3 is shown in Figure 4. The Pareto front of the test function ZDT3 is discontinuous and segmented, the non-inferior solution obtained by the traditional MOSPO algorithm (a) has the worst distribution uniformity and convergence in the spatial target, and the solution results of Improved-MOPSO(c) and the classical NSGA-II algorithm (b) are closer to the real Pareto frontier.

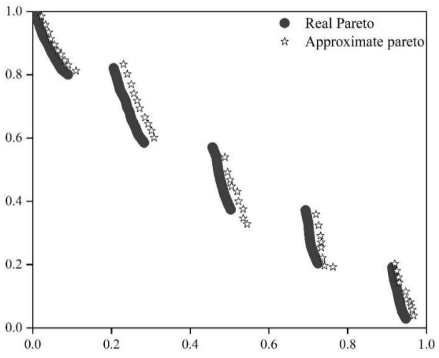

(a) MOPSO

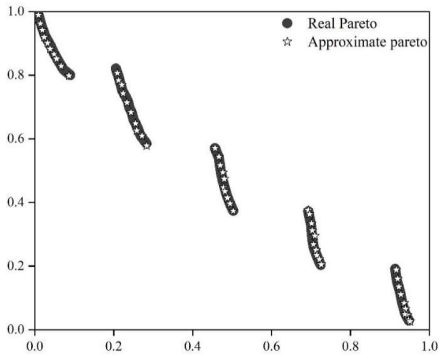

(b) NSGA-II

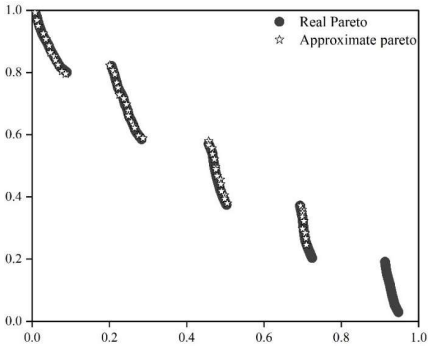

(c) Improved-MOPSO

Figure 4: The algorithm is near the edge of the pareto approximation on ZDT3

The Pareto approximation frontiers obtained by the three different algorithms on the test function ZDT4 are shown in Fig. 5. The Pareto frontiers of the test function ZDT4 contain more local extremes due to the different value ranges of the variables, and the distribution is similar to that of ZDT1. The algorithm (c) proposed in this paper outperforms the traditional MOPSO (a) and the classical NSGA-II algorithm (b) in terms of the effect of ZDT4 test function, has

the best ability to jump out of the local optimal solution, is closer to the real Pareto true frontier, and is suitable for solving the complex multi-objective optimization problems, whereas the MOSPO has poor convergence among the other algorithms.

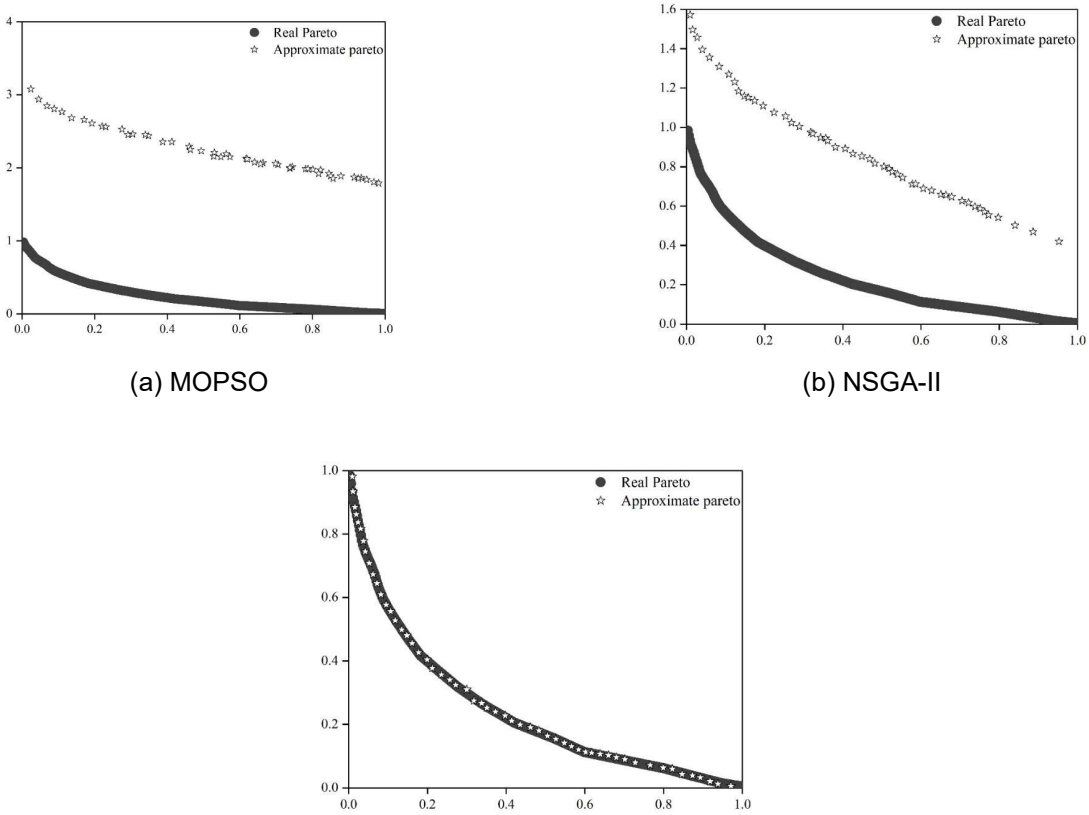

(a) MOPSO

(b) NSGA-II

(c) Improved-MOPSO

Figure 5: The algorithm is near the edge of the pareto approximation on ZDT4

In summary, the improved MOPSO algorithm has the best overall performance, and the solution set obtained from solving is closer to the real Pareto real frontier than other algorithms, with a more uniform distribution, better diversity, and the best ability to jump out of the local optimal solution, which is suitable for solving complex multi-objective optimization problems.

III. B. Example analysis

This chapter conducts a multi-storage configuration study for wind/photovoltaic/diesel/storage islanded grids, analyzes the results of multi-storage configuration from the perspectives of economy and voltage stability, respectively, and verifies the validity of the methodology.

III. B. 1) Economic analysis of optimized energy storage allocation

Wind and photovoltaic (PV) power generation are the main factors causing power fluctuations in the grid, and the comparison experiments in this section verify the importance of the energy storage system and the effectiveness of the optimal multi-storage allocation scheme proposed in this chapter, respectively. Three comparison scenarios are set up in the wind/photovoltaic/diesel/storage islanded grid. Scenario 1 has no energy storage equipment in the grid, Scenario 2 installs single storage in the grid, and Scenario 3 utilizes the multi-storage optimal configuration scheme proposed in this paper to configure multi-storage on seven alternative sensitive nodes (three nodes on the generation side, nodes 854, 852, and 832, and four nodes on the load side, nodes 834, 860, 836, and 838), and compares the grid system under different scenarios with nine joint wind/light estimated probability distributions, the calculation results are shown in Fig. 6.The point estimates of the 9 combined wind/photovoltaic power are shown in Table 4.

Table 4: Point Discrete Distribution of Wind/Solar Generation

Wind/light power(MW)	Probability(%)	Wind/light power(MW)	Probability(%)
0	7.63	0.64	7.13
0.16	5.31	0.86	9.63
0.26	35.42	1.02	6.34
0.38	1.63	1.24	1.93
0.42	24.36		

In Scenarios 2 and 3 with energy storage, with the increase of wind/photovoltaic output power, the operating cost of the grid is increased by the increase of operation and maintenance cost of PV, wind power generation and energy storage on the one hand, and on the other hand, due to the decrease of the consumption cost of fuel of traditional units, thus the operating cost is minimized when the output power of new energy reaches 0.86 MW. When the new energy output power is greater than 0.86MW, the fuel cost of the traditional unit is negligible, and the grid operation cost is mainly affected by the operation cost of PV, wind power generation and energy storage equipment, so it is approximately proportional to the new energy output. No energy storage system is installed in Scenario I, and the power fluctuation of the grid is all borne by the conventional unit, and the operating cost of Scenario I is the highest and the economy is the worst, with a cost as high as 58.6725$/h. Scenario II is configured with a single storage device, which bears a part of the power fluctuation but the operating cost is higher than that of the multi-storage system in Scenario III, and it can be seen that the optimal configuration of the multi-storage plan obtained by utilizing the methodology proposed in this paper is more conducive to the inclusion of the grid economic operation requirements of the new power system. Under the nine wind/light joint probability distribution estimation points, the cost of the multi-storage configuration scheme proposed in this paper is 54.3993$/h. It can be seen that the selection of this multi-storage configuration scheme can save about 37,433$ a year of operating cost in the grid containing new energy sources, which improves the economic operation of the power grid.

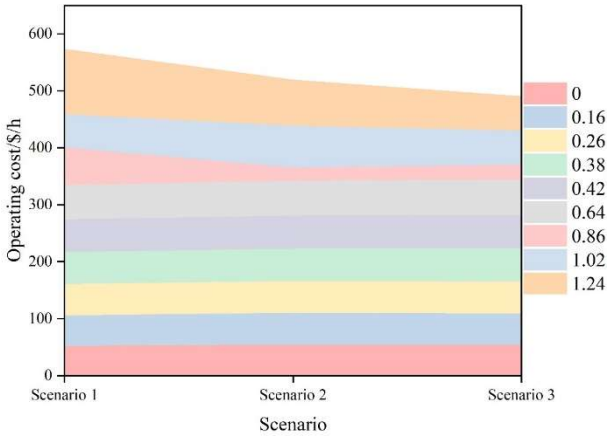

Figure 6: Total operation cost in three cases

III. B. 2) Voltage Stability Analysis for Optimized Energy Storage Configuration

This section analyzes the voltage stability of the energy storage configuration scheme, and the calculation results are shown in Fig. 7. With the increase of wind/light generation power, the amount of microgrid voltage fluctuation increases, especially in the microgrid without energy storage, the voltage fluctuation climbs sharply. Compared with the microgrid without energy storage, the voltage stability of the microgrid is improved after installing single energy storage, but it is difficult to ensure the stability of the single storage device in the region far away from the energy storage access node, and the multi-storage configuration scheme can most likely cover the stable operation of the whole power system, the voltage stability of the microgrid is improved by 77.96% after installing multi-storage, and the voltage fluctuation amount is only 0.28. Taking into account the stability of the operation of microgrid, the voltage stability of the selected multi-storage configuration scheme is improved by 77.96%. Considering the operational stability of the microgrid, the voltage stability of the multi-storage configuration is the best.

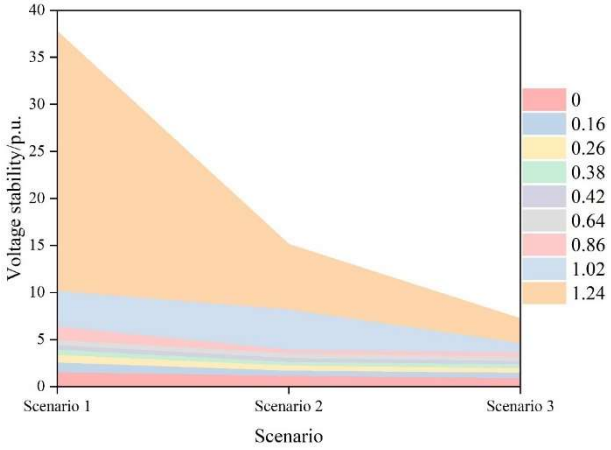

Figure 7: Voltage stability in three cases

III. B. 3) Design of energy storage network structure

While ensuring the stability of system operation, the optimal configuration of multiple energy storage proposed in this chapter effectively reduces the microgrid operation cost and voltage fluctuation amount. Considering the microgrid operation cost, carbon emission and voltage stability, nodes 834, 860, and 836 in the islanded grid of Fig. 1 are selected as the optimal installation nodes for three energy storage devices, and the storage sizes configured on each node are shown in Table 5.

Table 5: Optimal allocation of ESSs

Energy storage configuration scheme	834	860	836
Rated power(MW)	0.02	0.05	0.11
Capacity(MWh)	0.2	0.64	1.46

IV. Conclusion

The study adopts the improved MOPSO optimization algorithm to solve the mathematical model of optimal configuration of energy storage system. In order to verify the effectiveness of the proposed improved MOPSO algorithm and its performance advantages, the standard test functions ZDT1-ZDT4 are selected as test instances, and the distributions of the optimal solution sets obtained by different algorithms for solving the model are compared on the frontier solutions. The solution results of the improved MOPSO algorithm and the NSGA-II and MOSPO algorithms are evaluated by the multi-objective algorithm evaluation metrics generation distance (GD), spacing metric (SP) and inverse generation distance (IGD). The test results show that the improved MOPSO algorithm has the best overall performance and is suitable for solving complex multi-objective optimization problems. Using the constructed optimization model, the optimal access locations of energy storage are found to be nodes 834, 860, and 836 by analyzing the IEEE-34 node distribution system, and the multi-storage configuration is chosen to save about $37,433 a year of operating cost in the grid containing new energy sources, and the voltage stability can be improved by 77.96%. The reasonableness of the proposed model and algorithm in optimizing the energy storage network structure and improving the system stability is verified.

Acknowledgement

1. National Key R&D Program of China (No. 2023YFB2405900);
2. Inner Mongolia Electric Power (Group) Co., Ltd. Technology Project April 56, 2024.

References

[1] Ji, Z., Niu, D., Li, W., Wu, G., Yang, X., & Sun, L. (2022). Improving the energy efficiency of China: An analysis considering clean energy and fossil energy resources. Energy, 259, 124950.
[2] Payam, F., & Taheri, A. (2018). Challenge of fossil energy and importance of investment in clean energy in Iran. Journal of Energy Management and Technology, 2(1), 1-8.
[3] Kittner, N., Lill, F., & Kammen, D. M. (2017). Energy storage deployment and innovation for the clean energy transition. Nature Energy, 2(9), 1-6.
[4] Donnelly, K. B. (2023). Storing the future of energy: Navigating energy storage policy to promote clean energy generation. Environmental Progress & Sustainable Energy, 42(2), e14062.

[5] Wicki, S., & Hansen, E. G. (2017). Clean energy storage technology in the making: An innovation systems perspective on flywheel energy storage. Journal of cleaner production, 162, 1118-1134.
[6] Abdi, H., Mohammadi-ivatloo, B., Javadi, S., Khodaei, A. R., & Dehnavi, E. (2017). Energy storage systems. Distributed generation systems, 7, 333-368.
[7] Mohamad, F., Teh, J., Lai, C. M., & Chen, L. R. (2018). Development of energy storage systems for power network reliability: A review. Energies, 11(9), 2278.
[8] Arani, A. K., Karami, H., Gharehpetian, G. B., & Hejazi, M. S. A. (2017). Review of Flywheel Energy Storage Systems structures and applications in power systems and microgrids. Renewable and Sustainable Energy Reviews, 69, 9-18.
[9] Hemmati, R. (2018). Optimal design and operation of energy storage systems and generators in the network installed with wind turbines considering practical characteristics of storage units as design variable. Journal of Cleaner Production, 185, 680-693.
[10] Zame, K. K., Brehm, C. A., Nitica, A. T., Richard, C. L., & Schweitzer III, G. D. (2018). Smart grid and energy storage: Policy recommendations. Renewable and sustainable energy reviews, 82, 1646-1654.
[11] Li, X., & Wang, S. (2019). Energy management and operational control methods for grid battery energy storage systems. CSEE Journal of Power and Energy Systems, 7(5), 1026-1040.
[12] Rafaq, M. S., Basit, B. A., Mohammed, S. A. Q., & Jung, J. W. (2022). A comprehensive state‐of‐the‐art review of power conditioning systems for energy storage systems: Topology and control applications in power systems. IET Renewable Power Generation, 16(10), 1971-1991.
[13] Tur, M. R. (2020). Reliability assessment of distribution power system when considering energy storage configuration technique. IEEE Access, 8, 77962-77971.
[14] Aguado, J. A., de La Torre, S., & Triviño, A. (2017). Battery energy storage systems in transmission network expansion planning. Electric Power Systems Research, 145, 63-72.
[15] Datta, U., Kalam, A., & Shi, J. (2017, November). Battery energy storage system for transient frequency stability enhancement of a large-scale power system. In 2017 Australasian Universities Power Engineering Conference (AUPEC) (pp. 1-5). IEEE.
[16] Huang, P., Sun, Y., Lovati, M., & Zhang, X. (2021). Solar-photovoltaic-power-sharing-based design optimization of distributed energy storage systems for performance improvements. Energy, 222, 119931.
[17] Bozorg, M., Sossan, F., Le Boudec, J. Y., & Paolone, M. (2018). Influencing the bulk power system reserve by dispatching power distribution networks using local energy storage. Electric Power Systems Research, 163, 270-279.
[18] Zhang, S., Li, Y., Du, E., Fan, C., Wu, Z., Yao, Y., ... & Zhang, N. (2023). A review and outlook on cloud energy storage: An aggregated and shared utilizing method of energy storage system. Renewable and Sustainable Energy Reviews, 185, 113606.
[19] Sakipour, R., & Abdi, H. (2020). Optimizing battery energy storage system data in the presence of wind power plants: a comparative study on evolutionary algorithms. Sustainability, 12(24), 10257.
[20] Song, H., Liu, C., Amani, A. M., Gu, M., Jalili, M., Meegahapola, L., ... & Dickeson, G. (2024). Smart optimization in battery energy storage systems: An overview. Energy and AI, 100378.
[21] Zibo Xu & Yinsheng Ma. (2024). Configuration and Efficiency Mechanism Analysis of Ultra-High Temperature Heat Pump Energy Storage Systems for New Power Systems. International Journal of Heat and Technology,42(5).
[22] Koiwa Kenta,Ishii Tomoya,Liu Kang Zhi,Zanma Tadanao & Tamura Junji. (2019). On the Reduction of the Rated Power of Energy Storage System in Wind Farms. IEEE Transactions on Power Systems,35(4),1-1.
[23] Ikegami Takashi,Kataoka Kazuto,Iwafune Yumiko & Ogimoto Kazuhiko. (2013). Charging and Discharging Operation Algorithms of Home Storage Battery under Constraints of Reverse Power Flow from Residences with PV Systems. IEEJ Transactions on Electronics, Information and Systems,133(10),1884-1896.
[24] Ukoima Kelvin Nkalo,Okoro Ogbonnaya Inya,Obi, Patrick Ifeanyi,Akuru Udochukwu Bola & Davidson Innocent Ewean. (2024). A modified multi-objective particle swarm optimization (M-MOPSO) for optimal sizing of a solar–wind–battery hybrid renewable energy system. Solar Compass,12,100082-100082.
[25] Liang Dong & Jing Feng. (2022). Evaluation of Thermal Insulation Performance of Building Exterior Wall Based on Multiobjective Optimization Algorithm. Mobile Information Systems,2022.